Corrosion Behavior of Copper in 0.50 M Hydrochloric Acid Pickling Solutions and its Inhibition by 3-Amino-1,2,4-triazole and 3-Amino-5-mercapto-1,2,4-triazole

El-Sayed M. Sherif

Center of Excellence for Research in Engineering Materials (CEREM), College of Engineering, King Saud University, P. O. Box 800, Riyadh 11421, Kingdom of Saudi Arabia
*E-mail: esherif@ksu.edu.sa

The corrosion behavior of unalloyed copper (99.999% Cu) in freely aerated hydrochloric acid pickling, 0.50 M HCl, solutions and its inhibition by different concentrations of 3-amino-1,2,4-triazole (ATA) and 3-amino-5-mercapto-1,2,4-triazole (AMTA) were reported. The experiments have been carried out using weight-loss, potentiodynamic polarization (PDP), chronoamperometry (CA), electrochemical impedance spectroscopy (EIS), and Raman spectroscopy investigations. Weight-loss data indicated that copper dissolves rapidly in HCl solution due to the increased weight loss with increasing the exposure period. The addition of ATA and AMTA molecules to the acid solution remarkably decreased both the weight-loss and corrosion rate for copper; further decreases were obtained with the increase of these compounds concentrations due to the increase of their inhibition efficiencies. PDP, CA, and EIS measurements showed clearly that the presence of ATA and AMTA and the increase of their concentrations significantly decrease the corrosion reactions for copper in HCl solutions. The detection of ATA and AMTA molecules on the copper surface by Raman spectroscopy confirmed that the inhibition of copper corrosion in the acid solution is achieved by strong adsorption of these organic molecules onto the copper surface preventing the formation of cuprous chloride and oxy-chloride complex compounds.

1. INTRODUCTION

Copper is characterized by its high electrical and thermal conductivities and good mechanical workability. The metal has been widely used as a material in pipelines for domestic and industrial water utilities, heat conductors, heat exchangers, in electronic industries, and communications as a

conductor in electrical power lines. Corrosion products and deposited scales have a negative effect on heat transfer. This effect decreases the heating efficiency of the equipment and a periodic de-scaling and cleaning in hydrochloric acid pickling solutions are necessary. Thus, the corrosion of copper and its inhibition in hydrochloric acid solutions have been extensively studied by several researchers [1-8].

It has been reported that [5-17] anodic dissolution of copper in chloride media is influenced by the chloride concentration. At low chloride concentrations, the dissolution of copper occurs through formation of CuCl that transforms to the soluble $CuCl_2^-$ by reacting with excess chloride. While, at high concentrations, cuprous complexes such as $CuCl_3^{2-}$ and $CuCl_4^{3-}$ are formed, in addition to the ones with fewer chlorides such as *CuCl* and $CuCl_2^-$. The use of corrosion inhibitors is one of the most important methods to reduce the dissolution of copper is such corrosive environment [18]. In general, corrosion inhibitors are well known compounds to effectively eliminate the undesirable destructive effects of aggressive media and prevent metals and alloys dissolution. Especially those containing polar groups including nitrogen, sulfur and oxygen [19–21], and heterocyclic compounds with polar functional groups and conjugated double bonds [22–24] have been reported to inhibit copper corrosion. The inhibiting action of these inhibitors is usually attributed to their interactions with the metal/alloy surface via their adsorption [25, 26].

Organic compounds such as imidazole, benzimidazole, aminophenyl-tetrazole, n-phenyl-phenylenediamine, 2-amino-5-(ethylthio)-1,3,4-thiadiazole, benzothiazole and benzotriazole, contain nitrogen atoms, which coordinate with Cu(0), Cu(I) or Cu(II) through lone pair electrons to form complexes [2-7,9-11,27]. These complexes are believed to be polymeric in nature and form an adherent protective film on the copper surface, this film acts as a barrier to aggressive ions such as chloride [27]. Therefore, they have been reported to be good inhibitors against corrosion of copper in harsh environments, including chloride containing media.

The present work reports on the corrosion of copper after varied exposure periods in 0.50 M hydrochloric acid solutions and its inhibition by 3-amino-1,2,4-triazole (ATA) and 3-amino-5-mercapto-1,2,4-triazole (AMTA) . The chemical structure of ATA and AMTA are shown in Fig. 1a and Fig. 1b, respectively. ATA and AMTA were expected to be good inhibitors for copper corrosion in HCl solutions because they are heterocyclic compounds containing variety of donor groups; in addition, they are non-toxic and inexpensive. This work was performed using a variety of gravimetric, electrochemical and spectroscopic techniques.
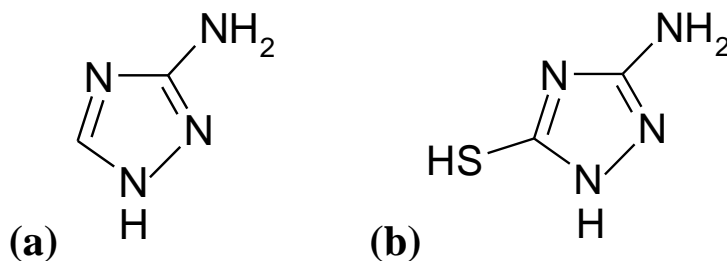
Figure 1. Chemical structure of (a) ATA and (b) AMTA.

2. EXPERIMENTAL PROCEDURE

2.1. Chemicals and electrochemical cell

Hydrochloric acid (HCl, Glassworld, 32%), 3-amino-1,2,4-triazole (ATA, Sigma-Aldrich, 95%), 3-amino-5-mercapto-1,2,4-triazole (AMTA, Sigma-Aldrich, 95%), and absolute ethanol (C_2H_5OH, Merck, 99.9%) were used as received. An electrochemical cell with a three-electrode configuration was used; a copper rod (Cu, Goodfellow, 99.999%, 5.0 mm in diameter), a platinum foil, and an Ag/AgCl electrode (in saturated KCl) were used as a working, counter, and reference electrodes, respectively. The copper rod for electrochemical measurements was prepared by welding a copper wire to a drilled hole was made on one face of the rod; the rod with the attached wire were then cold mounted in resin and left to dry in air for 24 h at room temperature. Before measurements, the other face of the copper rod, which was not drilled, was first grinded successively with metallographic emery paper of increasing fineness up to 800 grit and further polished with 5, 1, 0.50, and 0.30 mm alumina slurries (Buehler). The rod was then cleaned using doubly-distilled water, degreased with acetone, washed using doubly-distilled water again and finally dried with tissue paper.

2.2. Weight loss measurements

The weight loss experiments were carried out using rectangular copper coupons (Goodfellow, 99.999%) having the dimensions of 3.0 cm length, 1.0 cm width and 0.20 cm thickness with an exposed total area of 7.6 cm^2. The coupons were polished and dried as copper rods were, weighed (m_1), and then suspended in 100 cm^3 solution of 0.50 M HCl with and without the desired concentrations of ATA and AMTA for different exposure periods (6 – 48 h). At the end of a run, the samples were rinsed with distilled water, dried and weighed again (m_2). The loss in weight (Δm, $mg.m^{-2}$), the corrosion rate (K_{Corr}, $mg.m^{-2}.h^{-1}$), and the percentage of the inhibition efficiency (IE%) over the exposure time were calculated as previously reported in the previous work [28-33].

2.3. Electrochemical techniques

Electrochemical experiments were performed by using a Schlumberger SI-1286 electrochemical interface potentiostat-galvanostat. For potentiodynamic polarization experiments the potential was scanned from -500 to 250 mV vs. Ag/AgCl at a scan rate of 1 mV/s. Chronoamperometric current-time curves were obtained by setting the potential at 300 mV for 100 min. Impedance measurements were made using a Solatron SI 1255 HF frequency response analyzer along with the potentiostat-galvanostat. The instruments were controlled by the FRA-3.5 software program between 100 kHz and 0.05 Hz with an ac wave of ±5 mV peak-to-peak overlaid on a dc bias potential, and the impedance data were obtained at a rate of 10 points per decade change in frequency. All electrochemical measurements were carried out at an open circuit potential after varied immersion periods of 0 and 48 h of the copper electrode in the test electrolyte.

2.4. Raman spectroscopy investigations

Raman spectra were measured using a J-Y T64000 Raman spectrometer operated in single spectrograph mode with a holographic dispersive grating of 600grooves/mm giving a resolution of 2 cm^{-1}. The samples were analyzed in back-scattering mode on the microscope stage of Olympus confocal microscope attached to the spectrometer using a long working distance 20x objective. The detector used was a liquid nitrogen cooled charge coupled device (CCD) detector. A 647.1 nm holographic notch filter was used to remove the Rayleigh-scattered light. The entrance slit width was 100 μm.

3. RESULTS AND DISCUSSION

3.1. Weight-loss data

In order to study the corrosion of copper in 0.50 M HCl solutions and its inhibition by ATA and AMTA, gravimetric experiments were carried out. The variation of the weight loss versus time for copper coupons in 100 ml of 0.50 M HCl without (1) and with (2) 1.0×10^{-3} M ATA, (3) 5.0×10^{-3} M ATA, (4) 1.0×10^{-3} M AMTA, and (5) 5.0×10^{-3} M AMTA, respectively is shown in Fig. 2. It is seen from Fig. 2 (curves 1) that the weight-loss of copper in 0.50 M HCl solutions increases linearly with time as a result of the continuous dissolution of copper ions. At this condition the copper cations go to the solution (Eq. 1) and then react with chloride ions from the solution to form cuprous chloride (Eq. 2) on the copper surface. The formed CuCl does not give enough protection to the copper surface and transforms to the soluble copper chloride complex, $CuCl_2^-$ as can be seen from Eq. (3) [2-6, 12, 18],

$$Cu = Cu^+ + e^- \quad \text{(fast)} \qquad (1)$$

$$Cu^+ + Cl^- = CuCl \qquad (2)$$

$$CuCl + Cl^- = CuCl_2^- \qquad (3)$$

According to our previous work [2-6], if this formed $CuCl_2^-$ is adsorbed on the surface, its dissolution into the solution will go as follows,

$$CuCl_2^-{}_{(surface)} = CuCl_2^-{}_{(solution)} \qquad (4)$$

The formed $CuCl_2^-$ might further oxidize to cupric ions according to the reaction;

$$CuCl_2^-{}_{(surface)} = Cu^{2+} + 2Cl^- + e^- \qquad (5)$$

On the other hand, the presence of 1.0×10^{-3} M ATA (curve 2) considerably reduces the weight loss of copper and further decreasing in the loss of weight is greatly recorded by the increase of ATA concentration to 5.0×10^{-3} M. This is attributed to the adsorption of ATA molecules on the copper surface, which limits the dissolution of copper by blocking the corrosion sites and hence decreasing the weight-loss as its concentration increases. The presence of AMTA and the increase of its concentration provided even more protection to the copper surface and the dissolution of copper recorded minimum values over the 48 h time.
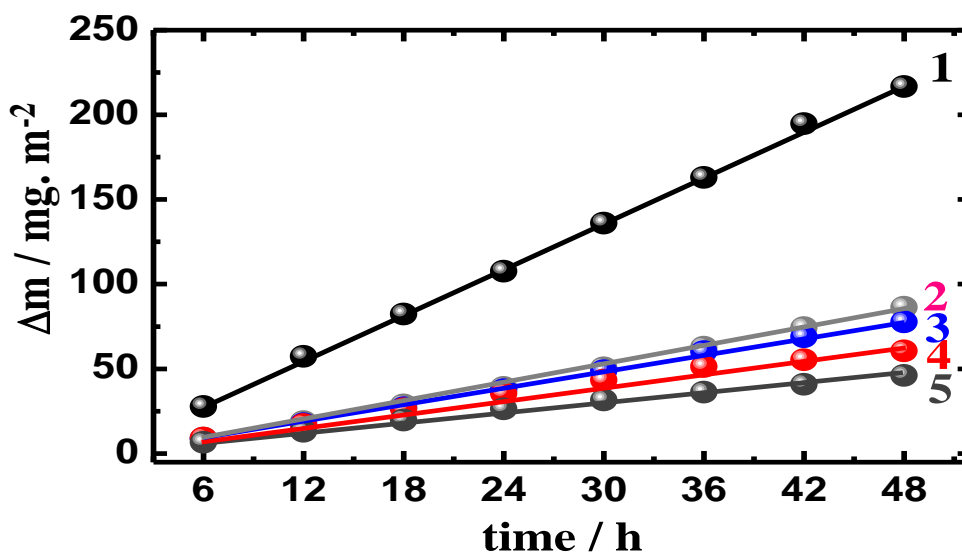
Figure 2. Change of the weight loss *(Δm)* versus time for copper coupons in 100 ml of 0.50 M HCl without (1) and with (2) 10^{-3} M ATA, (3) 5.0×10^{-3} M ATA, (4) 10^{-3} M AMTA, and (5) 5.0×10^{-3} M AMTA, respectively.
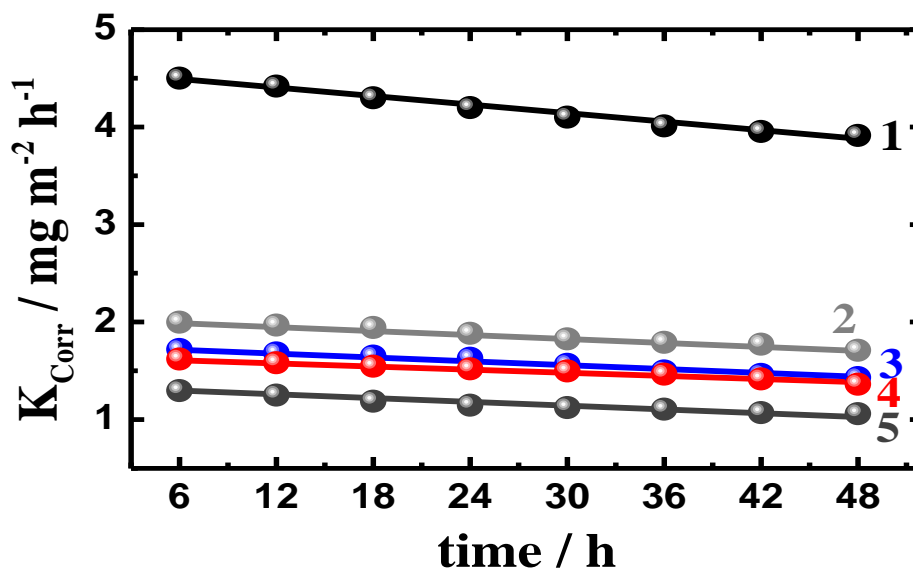
Figure 3. Change of the weight loss *(Δm)* versus time for copper coupons in 100 ml of 0.50 M HCl without (1) and with (2) 10^{-3} M ATA, (3) 5.0×10^{-3} M ATA, (4) 10^{-3} M AMTA, and (5) 5.0×10^{-3} M AMTA, respectively.

This was also confirmed by plotting the change of the corrosion rate (K_{Corr}) as a function of time for copper coupons in open to air 0.50 M HCl solutions without (1) and with (2) 1.0×10^{-3} M ATA, (3) 5.0×10^{-3} M ATA, (4) 1.0×10^{-3} M AMTA, and (5) 5.0×10^{-3} M AMTA, and the curves are shown respectively in Fig. 3. The K_{Corr} recorded higher values for copper in HCl alone, curve 1, due to the continuous attack on the copper surface; these values slightly decreased with increasing time. Addition of ATA and the increase of its concentration for a certain extent decreased values of K_{Corr} as a result of the adsorption of ATA molecules onto copper decreasing its dissolution in the test solution. The minimum K_{Corr} values were obtained for copper in the presence of AMTA molecules, curve 4 and curve 5.
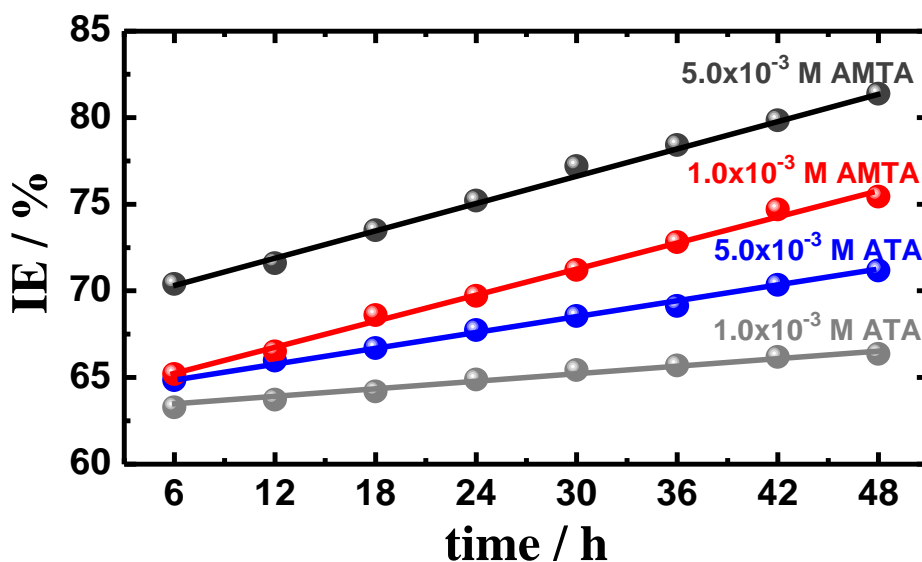
Figure 4. Variation of the inhibition efficiency obtained by weight-loss vs. time for copper coupons in aerated 0.50 M HCl containing 1.0×10^{-3} M and 5.0×10^{-3} M ATA and AMTA.

The percentage of the inhibition efficiency *(IE/%)* that was obtained from weight-loss data for copper surface by ATA and AMTA is plotted as a function of time as repersented in Fig. 4. It is clearly seen from Fig. 4 that the inhibition efficiency for copper by ATA and AMTA is increased by increasing their concentrations as well as the increase of the immersion time. The maximum *IE%* was obtained after 48 h and recorded 67% and 77% increased to 72% and 83% when the concentration was increased from 1.0×10^{-3} M to 5.0×10^{-3} M ATA and AMTA, respectively. This proves that the ability of AMTA as a corrosion inhibitor for copper in HCl test solution is higher than ATA at the same concentration. The presence of the mercapto group in the structure of AMTA molecule perhaps plays an important role in increasing its adsorption probability on the copper surface. This can be explained on the basis that sulfur containing compounds self-assemble on the surface of coinage metals such as copper, silver, and gold by forming strong covalent bonds between the sulfur atoms and the metal surface [34-37]. It has also reported that [38, 39] in aqueous acidic solution the triazole molecules get protonated and exist either as neutral molecules or in the form of cations. The protonated triazole

molecules may adsorb through electrostatic interaction between positively charged triazole molecules and negatively charged metal surface caused by chloride ions from the solution. While, neutral triazole molecules displace water molecules from the surface and share electrons with Cu surface. In both cases, the adsorbed film has hydrophobic action and protects the surface by blocking mainly the active sites on the copper surface [38]. The presence of S group in the triazole molecule also increases the number of lone pairs of electrons and higher the polarisability and then increases the adsorption probability of the AMTA molecules onto the copper surface [39].

3.2. Raman spectroscopy investigations

In order to see whether the ATA and AMTA molecules are indeed adsorbed onto copper surface, Raman spectroscopy investigations were performed. Fig. 5 shows the Raman spectra taken for the copper surface after its immersion for 48 h in (a) 0.50 M HCl + 5.0x10^{-3} M ATA and (b) 0.50 M HCl + 5.0x10^{-3} M AMTA, respectively. The Raman mode assignments for the copper surface shown in Fig. 5a are: 1006 cm^{-1} in-plane triazole ring stretching vibrations of ATA$^-$ anion interacting with Cu(I); 1035 cm^{-1} – N-N stretches; 1309 cm^{-1} – CH in plane bending; 1367 cm^{-1} – triazole ring stretching [37-39]. These characteristic bands confirm the presence of ATA or its complex with copper in the formed film. The peak at 1035 cm^{-1} can be unequivocally ascribed to the Cu–N stretching vibration due to the adsorption of ATA molecules onto the metallic copper [40].
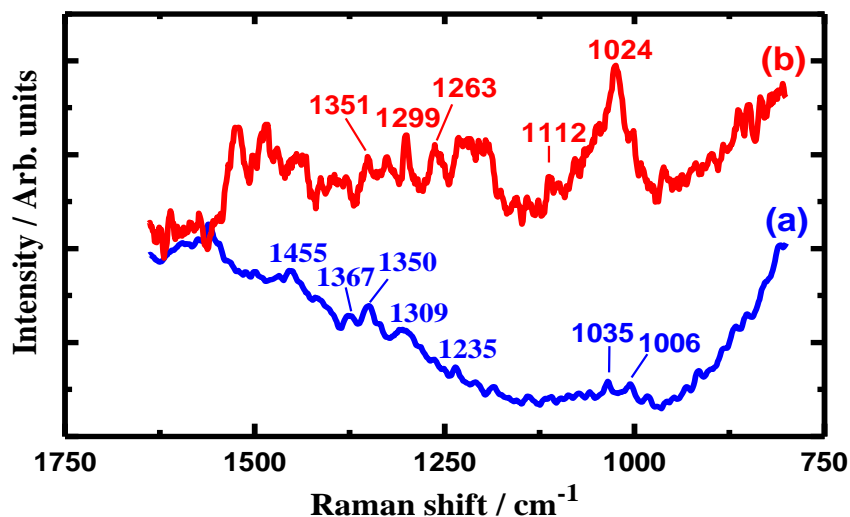
Figure 5. Raman spectra obtained on the copper surface after its immersion for 48 h in solution of 0.50 M HCl containing 5.0x10^{-3} M of (a) ATA and (b) AMTA respectively.

The Raman mode assignments found on the copper surface that was immersed for 48 h in 0.50 M HCl + 5.0x10^{-3} M AMTA as shown in Fig. 5b are: 1024.4 cm^{-1} can be unequivocally ascribed to the Cu–N stretching vibration due to the adsorption of AMTA molecules onto the metallic copper; 1112 cm^{-1} – in-plane N–H deformation; 1263 and 1299 cm^{-1} – in-plane C–H bending; 1351 cm^{-1} – triazole

ring stretching [40-42]. Thus, the characteristic bands found on the surface confirm the presence of AMTA or its complex with copper in the formed film. This emphasizes the hypothesis that the presence of either ATA or AMTA in the chloride solutions absorbs strongly on the copper surface, forms a complex with Cu^+ and then inhibits the copper corrosion by decreasing the formation of $CuCl_2^-$ through which the dissolution of copper occurs.

3.3. Potentiodynamic polarization (PDP) measurements

The PDP curves of the copper electrode in 0.50 M HCl solutions (1) without and with (2) $1.0x10^{-3}$ M and (3) $5.0x10^{-3}$ M of (a) ATA and (b) AMTA respectively are shown in Fig. 5. The cathodic reaction for copper surface in open to air 0.50 M HCl solutions is the oxygen reduction. This is because Cu is nobler than H^+ in the electromotive series, a cathodic reaction other than the displacement of H^+ must account for metal dissolution. This is readily available in terms of O_2 reduction from solution [5, 43],

$$O_2 + 4H^+ + 4\,e^- = 2H_2O \qquad\qquad (6)$$

It is clearly seen from Fig. 5 that the anodic currents display three distinct regions have reported in our previous work [2, 11]. These are, the Tafel region at lower over-potentials extending to the peak current density due to the fast dissolution of copper into Cu^+ (Eq. 1), this Cu^+ slowly oxidized to Cu^{2+} as follows,

$$Cu^+ = Cu^{2+} + e^- \text{ (slow)} \qquad\qquad (7)$$

Then, the region of decreasing currents until a minimum is reached due to the formation of CuCl (Eq. 2), due to the fast reaction of Cu^+ with Cl^- than Cu^{2+} does. The formation of corrosion products on the surface due to the hydrolysis of CuCl partially protects the copper and results in reducing the chloride ion attacks [2,3],

$$2CuCl + H_2O = Cu_2O + 2H^+ + 2Cl^- \qquad\qquad (8)$$

At last, the region of sudden increase in current density leading to a limiting value, which is due to the presence of acidic solutions decreases the adhesion properties of the adsorbed CuCl layer and leads to the formation of soluble copper chloride complex, $CuCl_2^-$ as represented by Eq. 3. It is believed that $CuCl_2^-$ is the responsible for copper corrosion and its dissolution into the bulk solution or its further oxidation to cupric ions [44] will occur as in Eq. 4 and Eq. 5, respectively.

The presence of $1.0x10^{-3}$ M ATA with the chloride solution as shown in Fig. 5a (curve 2) shifted the corrosion potential (E_{Corr}) to the more negative values and highly decreased the cathodic, corrosion current density (j_{Corr}), and anodic currents. This effect was greatly increased when the ATA concentration was increased to $5.0x10^{-3}$ M.
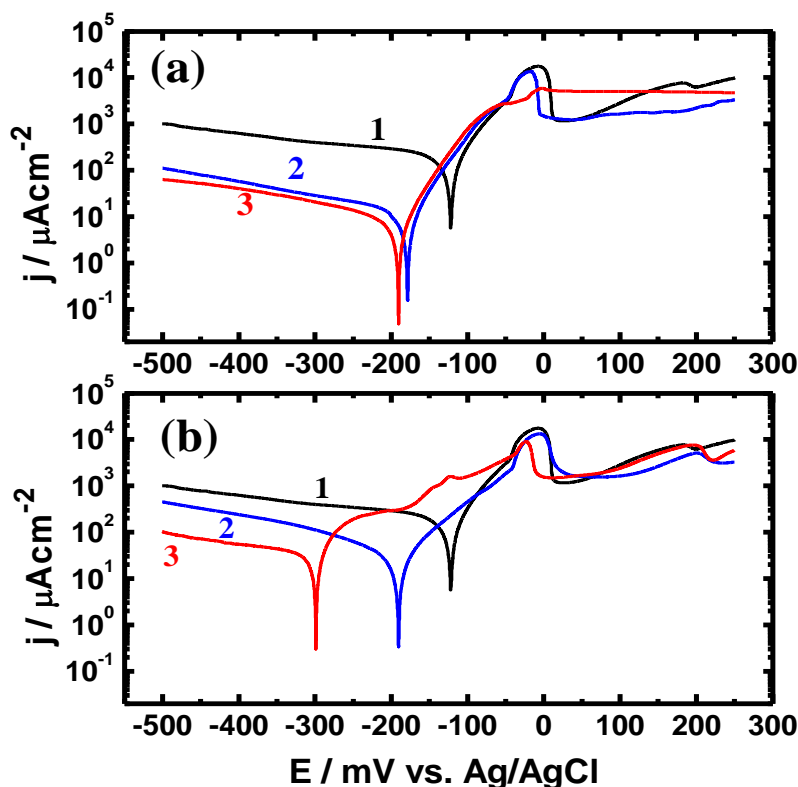
Figure 6. Potentiodynamic polarization curves for copper in 0.50 M HCl solutions without (1) and with (2) 1.0×10^{-3} M and (3) 5.0×10^{-3} M (a) ATA and (b) AMTA respectively.

The values of E_{Corr}, j_{Corr}, cathodic (β_c) and anodic (β_a) Tafel slopes, corrosion rate (K_{Corr}), polarization resistance (R_P), and the percentage of the inhibition efficiency *(IE%)* obtained from Fig. 5 are listed in Table 1. The calculations of all these parameters were made according to the previous work [45-50]. It is clear from Table 1 also that the presence of ATA and the increase of its concentration decreased K_{Corr} and increased R_P and IE% values. It is worth to mention also that the presence of AMTA and the increase of its concentration, Fig. 5b curve 2 and curve 3, gave similar effect to that obtained for ATA. The corrosion parameters obtained for Cu in HCl containing AMTA solutions are also listed in Table 1.

Table 1. Corrosion parameters obtained from PDP curves for copper electrode in 0.50 M HCl solutions in absence and presence of (ATA) and (AMTA), respectively

Solution	Parameter						
	E_{Corr}/ mV	j_{Corr}/ μA cm^{-2}	β_c/ mVdec^{-1}	B_a/ mVdec^{-1}	Rp/ kΩ	K_{Corr}/ Mpy	IE/ %
0.50 M HCl	-125	105.0	75	45	0.12	48.14	—
+1.0x10^{-3} M (ATA)	-185	13.50	85	50	1.03	6.19	87.1
+5.0x10^{-3} M (ATA)	-195	6.50	90	52	2.2	2.98	93.8
+1.0x10^{-3} M (AMTA)	-195	21.0	82	55	0.68	9.63	80.0
+5.0x10^{-3} M (AMTA)	-295	16.0	88	55	0.92	7.33	84.8

The decrease in j_{Corr} values is due to the decreased chloride ions attack on the copper surface by the increase of ATA and AMTA contents owing to the adsorption then polymerization of their molecules. The increase in β_c and β_a by the presence and the increase of the organic compounds concentration is mainly due to the decrease in both the cathodic and anodic currents, respectively. It has been reported [3, 51] that the variation in β_c and β_a values results from the change in the rate of copper electrodissolution particularly at high inhibitor concentrations; in spite dissolution via two electron reactions, copper undergoes one-electron oxidation primarily to Cu^+ in the presence of ATA and AMTA and form insoluble complex with copper on the surface. The decrease of K_{Corr} and the increase of R_P by ATA and AMTA indicate that ATA and AMTA suppress copper corrosion via their adsorption then polymerization onto the surface. The increase of *IE%* also confirms that ATA and AMTA at the tested concentrations are good inhibitors for copper surface in acidic chloride solutions.

3.4. Chronoamperometric current-time measurements

In order to study effects of the organic compounds on the corrosion inhibition of copper at more positive potentials, chronoamperometric current-time experiments were carried out at 300 mV vs. Ag/AgCl. The change of the dissolution currents as a function of time for copper electrode at 300 mV vs. Ag/AgCl in 0.50 M HCl solutions containing (1) 0.0 M, (2) 1.0×10^{-3} M and (3) 5.0×10^{-3} M of (a) ATA and (b) AMTA, respectively is shown in Fig. 7.
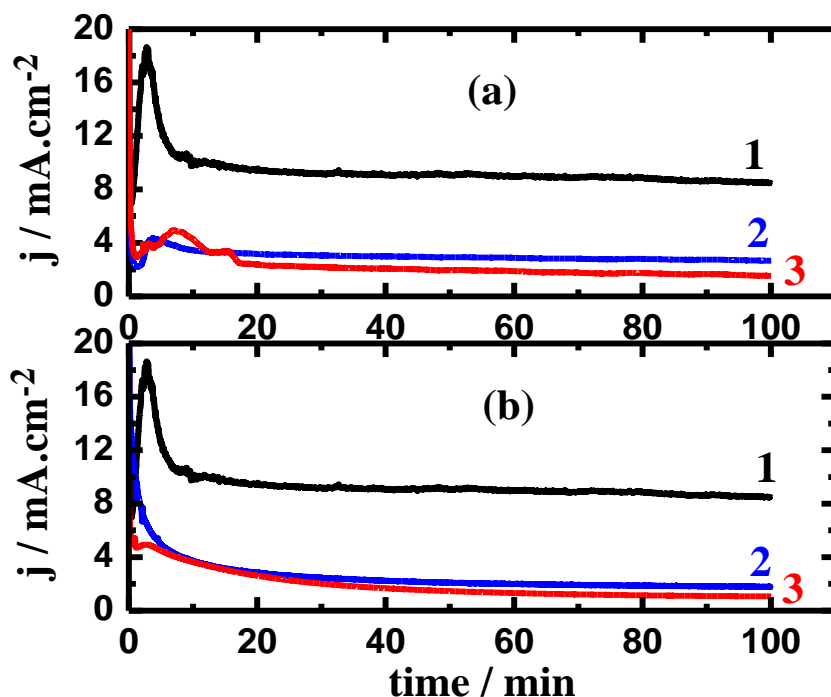
Figure 7. Chronoamperometric current-time curves obtained at 300 mV vs. Ag/AgCl for copper in 0.50 M HCl solutions without (1) and with (2) 1.0×10^{-3} M and (3) 5.0×10^{-3} M of (a) ATA and (b) AMTA respectively.

It is shown from Fig. 7, curves 1, that the current rapidly increased in the first few minutes and upon the application of the constant potential, which is due to the dissolution of copper according to Eq. (1). The current then decreased as a result of the partial protection provided for the surface by the formation of CuCl, Eq. (2). It has been reported that the corrosion products formed on the surface at the same conditions can be CuCl that transferred to $CuCl_2^-$, Eq. (3) [6]. The presence of $CuCl_2^-$ on copper reveals that the surface is not protected and explains the highest absolute currents obtained for copper in the absence of any inhibitors.

The presence of $1.0x10^{-3}$ M ATA, Fig. 7a curve 2, decreased the dissolution currents for the whole time of the experiment and further decreases in currents were observed upon increasing the ATA concentration to $5.0x10^{-3}$ M. This effect was also increased for copper in the presence of the same concentrations of AMTA, Fig. 7b curves 2 and 3. This agrees with the data obtained from polarization curves shown in Fig. 6 and is probably due to the adsorption then polymerization of the organic molecules to form a thick massive layer, which could be seen with naked eye on the copper surface preventing it from being corroded easily. This also confirms that AMTA provides better inhibition for copper corrosion in HCl solutions compared to ATA at the same concentration.

3.5. Electrochemical impedance spectroscopy (EIS) measurements

EIS is a powerful technique that has been successfully employing to explain corrosion mechanisms and adsorption phenomena [45-59].
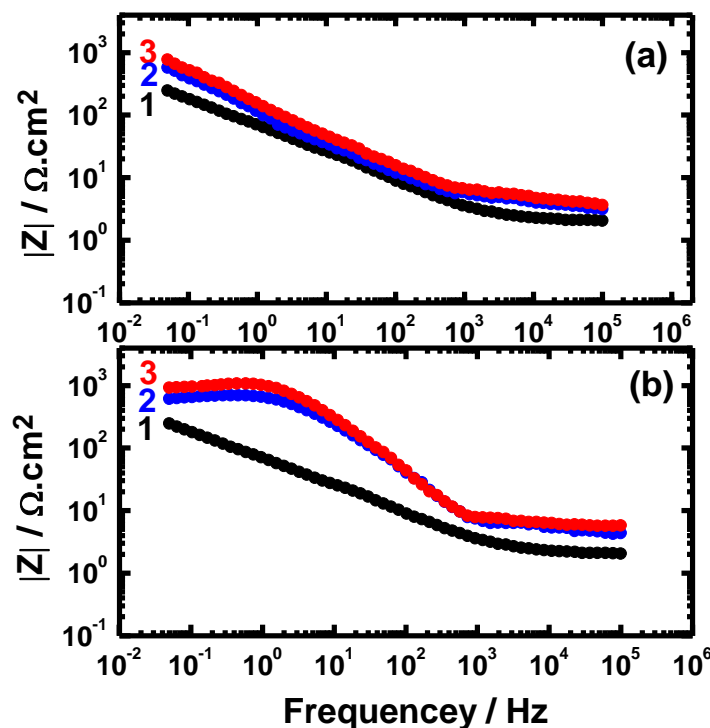
Figure 8. Bode plots obtained at open circuit potential for copper in 0.50 M HCl solutions without (1) and with (2) $1.0x10^{-3}$ M and (3) $5.0x10^{-3}$ M of (a) ATA and (b) AMTA present, respectively.

Fig. 8 shows the Bode EIS plots of the copper electrode in 0.50 M HCl solutions without (1) and with (2) 1.0×10^{-3} M and (3) 5.0×10^{-3} M of (a) ATA and (b) AMTA respectively. It can be seen from Fig. 8 that the impedance of the copper in chloride solution alone, curves 1, recorded lower values at the high frequency values and then increased with decreasing the frequency. In the presence of 1.0×10^{-3} M ATA, Fig. 8a (curve 2) greatly raised the impedance values over the whole frequency range. This effect was further increased with increasing the concentration of ATA to 5.0×10^{-3} M, Fig. 8a, curve 3. In respect to the Bode plots in the presence of AMTA, Fig. 8b curve 2 and curve 3, the impedance recorded the highest values over the full frequency range compared to the obtained ones for copper either in the absence or the presence of ATA molecules.

It has reported [55] that the higher the impedance at low frequencies the higher the passivation of the surface against corrosion. This means that ATA and AMTA molecules have the ability to inhibit the corrosion of copper in the HCl test solution and AMTA is having higher inhibition efficiency compared to ATA as the same concentration. This also agrees with the data obtained from weight-loss, polarization and chronoamperometric experiments and gives further confirmation of the ability of ATA and AMTA to highly protect the copper surface against corrosion in 0.50 M HCl solutions.

4. CONCLUSIONS

The corrosion of copper in 0.50 M HCl solutions and its inhibition by ATA and AMTA molecules have been investigated using a variety of gravimetric, electrochemical, and spectroscopic techniques. The outcome results can be summarized as follows:

❖   Weight-loss data showed that the presence of ATA and AMTA significantly inhibit the severe copper corrosion in HCl solutions: this effect increases with the increase of their concentrations.

❖   Raman spectra that were taken on copper after its immersion for 48 h in HCl containing 5.0×10^{-3} M of the used inhibitors confirmed the adsorption of ATA and AMTA molecules on the surface.

❖   Potentiodynamic polarization measurements indicated that the increased concentrations of ATA and AMTA decrease the cathodic, j_{Corr} and anodic currents and K_{Corr}, while increase β_c, β_a, and R_P.

❖   Chronoamperometric current-time experiments at 300 mV vs. Ag/AgCl for 100 min revealed that the dissolution of Cu greatly decreases as a result of the organic molecules thanks to their adsorption on the copper surface forming a protective layer and preventing the formation of cuprous chloride and oxychloride complexes.

❖   EIS Bode curves for copper in the presence of the ATA and AMTA recorded the highest impedance values over the full frequency range compared to the obtained ones for copper in chloride solutions alone.

❖   Results together are internally consistent with each other, showing that ATA and AMTA are good corrosion inhibitors for copper in 0.50 M HCl; they inhibit the corrosion by the strong adsorption of their molecules to form a complex with the copper surface and the inhibition efficiency of AMTA is higher than ATA due to the presence of an S group in the AMTA structure.

References

1. M.M. Antonijevic, M.B. Petrovic, *Int. J. Electrochem. Sci.,* 3 (2008) 1-28.
2. E.M. Sherif, S.-M. Park, *Electrochim. Acta,* 51 (2006) 4665.
3. E.M. Sherif, S.-M. Park, *Electrochim. Acta,* 51 (2006) 6556.
4. El-Sayed M. Sherif, R.M. Erasmus, J.D. Comins, *J. Colloid & Inter. Sci.* 306 (2007) 96.
5. El-Sayed M. Sherif, R.M. Erasmus, J.D. Comins, *Corros. Sci.,* 50 (2008) 3439.
6. El-Sayed M. Sherif, *J. Mater. Eng. Perform.,* 19 (2010) 873.
7. El-Sayed M. Sherif, *Int. J. Electrochem. Sci.,* 7 (2012) 1482.
8. Maqsood Ahmad Malik, Mohd Ali Hashim, Firdosa Nabi, Shaeel Ahmed AL-Thabaiti, Zaheer Khan, *Int. J. Electrochem. Sci.,* 6 (2011) 1927.
9. El-Sayed M. Sherif, *J. Appl. Surf. Sci*., 252 (2006) 8615.
10. El-Sayed M. Sherif, A.A. Almajid, *J. Appl. Electrochem*., 40 (2010) 1555.
11. E.M. Sherif, S.-M. Park, *J. Electrochem. Soc.*, 152 (2005) B428.
12. A.El Warraky, H.A. El Shayeb, E.M. Sherif, *Anti-Corros. Methods Mater.*, 51 (2004) 52.
13. M.M. Antonijevic, S.C. Alagic, M.B. Petrovic, M.B. Petrovic, M.B. Radovanovic, A.T. Stamenkovic, *Int. J. Electrochem. Sci.,* 4 (2009) 516.
14. L. Bacarella, J. C. Griess, *J. Electrochem. Soc.*, 120 (1973) 459.
15. H. P. Lee and K. Nobe, *J. Electrochem. Soc.*, 133 (1986) 2035.
16. M.M. Antonijevic, S.M. Milic, M.D. Dimitrijevic, M.B. Petrovic, M.B. Radovanovic, A.T. Stamenkovic, *Int. J. Electrochem. Sci.,* 4 (2009) 962.
17. S.M. Milic, M.M. Antonijevic, *Corros. Sci.,* 51 (2009) 28.
18. D-Q. Zhang, L-X. Gao, and G-D. Zhou, *J. Appl. Surf. Sci.,* 225 (2004) 287.
19. H. Ma, S. Chen, L. Niu, S. Zhao, S. Li, D. Li, *J. Appl. Electrochem.,* 32 (2002) 65.
20. H. Otmaĉiĉ, J. Telegdi, K. Papp, E. Stupnisek-Lisac, *J. Appl. Electrochem.,* 34 (2004) 545.
21. El-Sayed M. Sherif, A.M. El-Shamy, M.M. Ramla, A.O.H. El-Nazhawy, *Mater. Chem. Phys.,* 102 (2007) 231.
22. E.M. Sherif, S.-M. Park, *Corros. Sci.,* 48 (2006) 4065.
23. El-Sayed M. Sherif, R.M. Erasmus, J.D. Comins, *J. Appl. Electrochem*., 39 (2009) 83.
24. El-Sayed M. Sherif, A.Y. Ahmed, *Synthesis and Reactivity in Inorganic, Metal-Organic, and Nano-Metal Chemistry,* 40 (2010) 365.
25. M. G. Fontana, and K. W. Staehle, *"Advances in Corrosion Science and Technology"*, Vol. 1, Plenum Press, New York, 1970.
26. O. L. Riggs Jr., *"Corrosion Inhibitors",* 2nd ed., Nathan, C. C., Houston, TX, 1973.
27. V. Lakshminarayanan, R. Kannan, S.R. Rajagopalan, *J. Electroanal. Chem.,* 364 (1994) 79.
28. El-Sayed M. Sherif, J.H. Potgieter, J.D. Comins, L. Cornish, P.A. Olubambi, C.N. Machio, *J. Appl. Electrochem.,* 39 (2009) 1385.
29. El-Sayed M. Sherif, J.H. Potgieter, J.D. Comins, L. Cornish, P.A. Olubambi, C.N. Machio, *Corros. Sci.,* 51 (2009) 1364.
30. El-Sayed M. Sherif, A.A. Almajid, A.K. Bairamov, Eissa Al-Zahrani, *Int. J. Electrochem. Sci.,* 6 (2011) 5430.
31. El-Sayed M. Sherif, *Int. J. Electrochem. Sci.,* 6 (2011) 5372.
32. El-Sayed M. Sherif, *Int. J. Electrochem. Sci.,* 6 (2011) 2284.
33. El-Sayed M. Sherif, A.A. Almajid, *Int. J. Electrochem. Sci.,* 6 (2011) 2131.
34. F. Matsumoto, M. Ozaki, Y. Inatomi, S.C. Paulson, N. Oyama, *Langmuir,* 15 (1999) 857.

35. T.P. Ang, T.S.A. Wee, W.S. Chin, *J. Phys. Chem. B,* 108 (2004) 11001.
36. F. Bussolotti, S. D'Addato, F. Allegretti, V. Dhanak, C. Mariani, *Surf. Sci.,* 578 (2005) 136.
37. V.D. Castro, F. Bussolotti, C. Mariani, *Surf. Sci.,* 598 (2005) 218.
38. P.G. Fox, P.A. Bradely, *Corros. Sci.,* 20 (1980) 643.
39. A.Lalitha, S. Ramesh, S. Rajeswari, *J. Electrochim. Acta,* 51 (2005) 47.
40. Marek Graff, Jolanta Bukowska, Katarzyna Zawada, *J. Electroanal. Chem.,* 567 (2004) 297.
41. V. Oteino-Alego, N. Huynh, T. Notoya, S.E. Bottle, D.P. Schweinsberg, *Corros. Sci.,* 41 (1999) 685.
42. P.G. Cao, J.L. Yao, J.W. Zheng, R.A. Gu, Z.Q. Tian, *Langmuir,* 18 (2002) 100.
43. A.M. Shams E1 Din, M.E. E1 Dahshan, A.M. Taj E1 Din, *Desalination,* 130 (2000) 89.
44. M. Braun and K. Nobe, *J. Electrochem. Soc.,* 126 (1979) 1666.
45. El-Sayed M. Sherif, *Int. J. Electrochem. Sci.,* 6 (2011) 3077.
46. El-Sayed M. Sherif, A.A. Almajid, F.H. Latif, H. Junaedi, *Int. J. Electrochem. Sci.,* 6 (2011) 1085.
47. El-Sayed M. Sherif, *Mater. Chem. Phys.,* 129 (2011) 961.
48. El-Sayed M. Sherif, *Int. J. Electrochem. Sci.,* 6 (2011) 1479.
49. K.A. Khalil, El-Sayed M. Sherif, A.A. Almajid, *Int. J. Electrochem. Sci.,* 6 (2011) 6184.
50. F.H. Latief, El-Sayed M. Sherif, A.A. Almajid, H. Junaedi, *J. Anal. Appl. Pyrolysis,* 92 (2011) 485.
51. E.M. Sherif, S.-M. Park, *J. Electrochem. Soc*., 152 (2005) B205.
52. E.M. Sherif, S.-M. Park, *Electrochim. Acta,* 51 (2006) 1313.
53. K.F. Khaled, N. Hackerman, *Electrochim. Acta,* 49 (2004) 485.
54. El-Sayed M. Sherif, R.M. Erasmus, J.D. Comins, *Electrochim. Acta*, 55 (2010) 3657.
55. F. Mansfeld, S. Lin, S. Kim, H. Shih, *Corros. Sci.,* 27 (1987) 997.
56. El-Sayed M. Sherif, R.M. Erasmus, J.D. Comins, *Colloid Interface Sci.,* 309 (2007) 470.
57. El-Sayed M. Sherif, Corrosion of Duplex Stainless Steel Alloy 2209 in Acidic and Neutral Chloride Solutions and its Passivation by Ruthenium as an Alloying Element, *Int. J. Electrochem. Sci.,* 7 (3) (2012) in press.
58. J.H. Potgieter, P.A. Olubambi, L. Cornish, C.N. Machio, El-Sayed M. Sherif, *Corros. Sci*., 50 (2008) 5272.
59. El-Sayed M. Sherif, R.M. Erasmus, J.D. Comins, *Colloid Interface Sci.*, 311 (2007) 144.